Orbital-Symmetry-Dependent Electron Transfer through Molecules Assembled on Metal Substrates

ARTICLE *in* JOURNAL OF PHYSICAL CHEMISTRY LETTERS · JANUARY 2012

Impact Factor: 7.46 · DOI: 10.1021/jz2015567

THE JOURNAL OF PHYSICAL CHEMISTRY Letters

Letter

pubs.acs.org/JPCL

Orbital-Symmetry-Dependent Electron Transfer through Molecules Assembled on Metal Substrates

Florian Blobner,*[,†] Pedro B. Coto,*[,‡] Francesco Allegretti,[†] Michel Bockstedte,[‡] Oscar Rubio-Pons,[‡,¶] Haobin Wang,[§] David L. Allara,[∥] Michael Zharnikov,[⊥] Michael Thoss,[‡] and Peter Feulner[†]

[†]Physik-Department E20 and [¶]Department Chemie, Lehrstuhl für Theoretische Chemie, Technische Universität München, 85748 Garching, Germany

[‡]Institut für Theoretische Physik und Interdisziplinäres Zentrum für Molekulare Materialien, Friedrich-Alexander-Universität Erlangen-Nürnberg, 91058 Erlangen, Germany

[§]Department of Chemistry and Biochemistry, MSC 3C, New Mexico State University, Las Cruces, New Mexico 88003, United States

[∥]Departments of Chemistry and Material Science, Pennsylvania State University, University Park, Pennsylvania 16802, United States

[⊥]Angewandte Physikalische Chemie, Universität Heidelberg, 69120 Heidelberg, Germany

Supporting Information

ABSTRACT: Femtosecond charge-transfer dynamics in self-assembled monolayers of cyano-terminated ethane-thiolate on gold substrates was investigated with the core hole clock method. By exploiting symmetry selection rules rather than energetic selection, electrons from the nitrogen K-shell are state-selectively excited into the two symmetry-split π^* orbitals of the cyano end group with X-ray photons of well-defined polarization. The charge-transfer times from these temporarily occupied orbitals to the metal substrate differ significantly. Theoretical calculations show that these two π^* orbitals extend differently onto the alkane backbone and the anchoring sulfur atom, thus causing the observed dependence of the electron-transfer dynamics on the symmetry of the orbital.

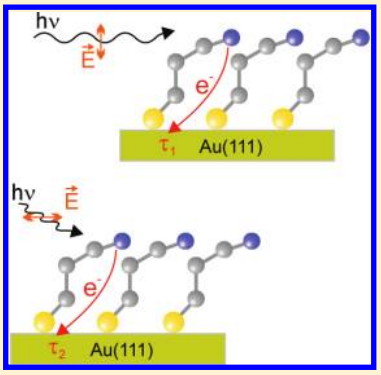

SECTION: Electron Transport, Optical and Electronic Devices, Hard Matter

Since the pioneering electron paramagnetic resonance (EPR) experiments of Weissman[1] and Voevodskij et al.[2] on intramolecular charge exchange and the related theoretical interpretation by McConnell,[3] charge transport through molecular entities and its microscopic details have attracted continuously increasing interest due to their fundamental importance for many fields and applications. Important examples include (i) electron-transfer (ET) and redox reactions in chemistry, electrochemistry, and biology;[4−6] (ii) materials modification by electronic excitations,[7] including irradiation-induced tailoring of thin organic films[8] and beam effects in spectroscopy and microscopy;[9] (iii) molecular photovoltaics;[10,11] and (iv) the field of molecular electronics.[12] The most direct access to charge transport through molecules is certainly by making contact either to single molecules or groups of molecules and measuring current versus voltage (I−V) curves (see ref 13 for a review of connection techniques). Extensive theoretical work is available for the interpretation of such I−V results.[12,14] Further detailed insight is obtained from the analysis of fluctuations of the electrical current and the study of inelastic processes such as current-induced vibrational and conformational excitations.[12,15,16]

The EPR studies mentioned above, however, belong to a different class of experiments. There, spectroscopic features related to an intrinsic time scale are analyzed. The EPR spectra from an uncompensated electron spin in anions consisting of two aromatic rings connected either by one[2] or two[1] aliphatic chains show hyperfine interaction with either one or both rings or an intermediate signature, depending on the electron exchange rate as a function of chain length. In these experiments, the limiting time resolution was the inverse frequency of the hyperfine interaction in the 0.1−1 μs range,[1,2] that is, the method is appropriate for slow transfer. To track faster processes, a shorter time interval reference is required, and as such, the lifetime of inner shell vacancies[17] proved to be valuable. By this core hole clock method (CHC), the transfer dynamics of an electron resonantly excited from an inner shell is obtained from the ratio of resonant and nonresonant core decay spectra in combination with the known lifetimes of core holes.[18,19] In most cases, the delocalization time of the resonantly excited core electron into a continuum, that is, the conduction band of a metallic substrate or another conductor, during the lifetime of the core hole is recorded; the inverse

Received: November 25, 2011
Accepted: January 17, 2012
Published: January 17, 2012

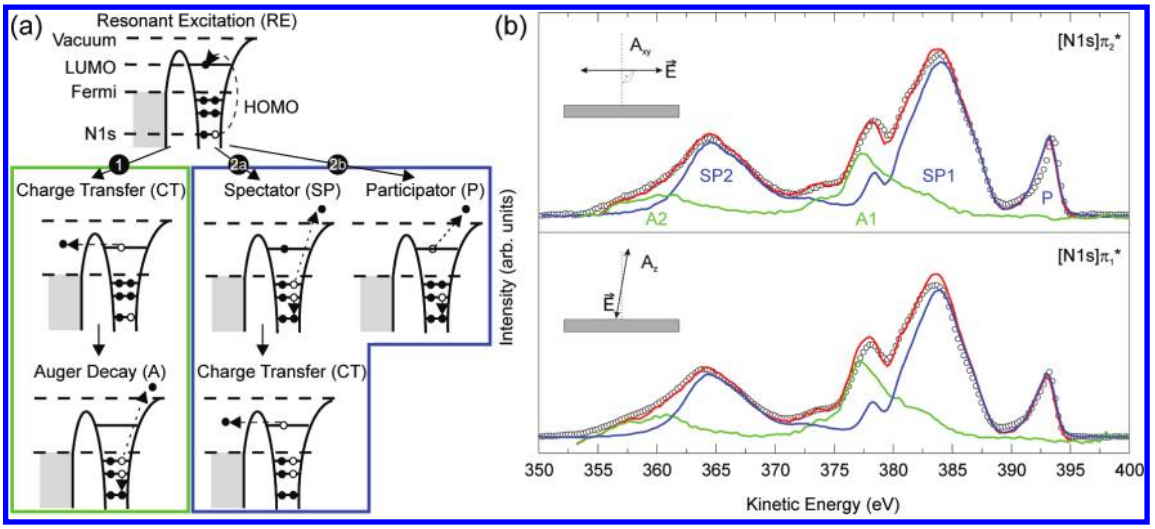

Figure 1. (a) Schematic of core excitation and de-excitation pathways for a molecule coupled to a continuum. Following resonant excitation, nonresonant (1) and resonant (2a,2b) pathways exist for the de-excitation, resulting in distinguishable decay electron spectra. (b) CHC evaluation of data sets for A_{xy} (top) and A_z light (bottom). The experimental decay spectra obtained from C2CN samples at resonance (black points) are reproduced by a linear combination (red line) of the nonresonant line shape recorded for C2CN above resonance (green line) and a purely resonant decay spectrum from C16CN (blue line). Photoemission contributions from the Au substrate and the organic layer have been determined by measurements in the pre-edge range and subtracted.

process, that is, the promotion of an electron from the continuum toward the core ionized atom before core decay, is however possible as well.[19] Despite its limitations due to the "availability" of core levels and resonances with appropriate lifetimes and energies, respectively, the CHC method has the advantage that it represents an atom-selective probe of the electron relaxation dynamics.[18−21] It was used by some of us for investigations of charge transport in thiolate-bonded self-assembled monolayers (SAMs) with aliphatic[22,23] and aromatic as well as mixed aliphatic/aromatic backbones.[24,25] We demonstrated that CHC is well-suited for the investigation of charge-transport dynamics through the backbones as well as through the anchor of the SAMs, yielding data corroborating and supplementing results from theory and $I-V$ conductance measurements.[22−25] In addition, we could show that ET from a core-excited N atom in a cyano (CN) substituent group through an adjacent aromatic backbone and into the substrate can depend strongly on the orbital to which the core electron has been primarily promoted. In a CN group attached to an aromatic ring, the π^* degeneracy is lifted, yielding in-plane and out-of-plane [N1s]π^* resonances. By selective excitation of these resonances (their excitation energies differ by 0.95 eV[25]), we found much faster charge transfer for the out-of-plane π^* orbital, which is strongly coupled to the aromatic π system,[25] relative to the in-plane orbital, which is not π-coupled. In the present work, we show that a similar symmetry-dependent effect exists for aliphatic CN-terminated SAMs as well. This is remarkable because for these systems, the effect of symmetry breaking is much weaker: The energy separation of the two [N1s]π^* resonances of the CN ligand at 399.6 and 399.7 eV, that is, 1.1 and 1.2 eV above the Fermi edge, is nearly an order of magnitude smaller than their spectral widths,[22,23] and selective ET into one of the two unoccupied orbitals simply by selecting the correct photon energy is impossible. Instead, by applying an approach developed for CHC experiments on atomic adsorbates,[26] we use the well-defined polarization of soft X-ray photons from a synchrotron storage ring for orbital-selective excitation. We believe that at present, CHC is the only method enabling such an orbital *and* site-selective look of charge-transport processes as reported here.

In Figure 1a, the schematic of core excitation and de-excitation routes in a molecule coupled to a continuum shows the essential basis for evaluating the decay spectra in the framework of the CHC method. First, a core electron (N1s) is promoted by synchrotron radiation to an unoccupied bound state above the Fermi level. The subsequent decay of the core hole can take place *before* or *after* the transfer of the resonantly excited electron to the substrate continuum. Because the resulting decay spectra differ for decay events before and after delocalization of the charge, measured data containing contributions from both routes can be decomposed into purely resonant (decay before delocalization) and purely nonresonant (decay after delocalization) fractions.

In the nonresonant case (route 1 in Figure 1), the final state is a two-hole (2h) state that corresponds to normal Auger decay (A), whereas in the resonant case, two possible pathways (routes 2a and 2b) for core decay exist. On the one hand, the electron in the resonance can participate in the decay; then, the final state is a 1h state which is labeled participator decay (P). If the electron, on the other hand, does not participate in the core hole decay, the final state becomes a two-hole one-electron (2h1e) state, hence called spectator decay (SP).

To allow for decomposition of the resonant decay spectrum into resonant and nonresonant contributions, pure resonant and pure nonresonant spectra have to be acquired. The pure nonresonant ($S_{nonresonant}$) spectrum is obtained by excitation above the resonance threshold, corresponding to normal Auger decay, whereas resonant excitation of a similar system where charge transfer does not take place yields a pure resonant spectrum ($S_{resonant}$). Reproducing the experimentally obtained resonant decay spectrum by a linear combination of $S_{resonant}$ and $S_{nonresonant}$ allows the calculation of the charge-transfer time according to the CHC framework using the expression $\tau_{CT} = \tau_{core}(I_{resonant}/I_{nonresonant})$,[19] where τ_{core} is the core hole lifetime and the I terms are the respective weights of the linear combination.

dx.doi.org/10.1021/jz2015567 | J. Phys. Chem. Lett. 2012, 3, 436−440

We performed our experiment with thiolate-bonded Au−S−$(CH_2)_2$−CN and Au−S−$(CH_2)_{16}$−CN SAMs, abbreviated as C2CN and C16CN. They have been prepared by a standard immersion procedure[27] on Au(111) substrates (with randomly oriented domains) evaporated (100 nm) on Si(111) wafers primed with a thin (5 nm) Ti layer to improve adhesion. Experiments were performed at the HESGM beamline of the synchrotron radiation facility BESSY II, Berlin. For nearly noise free decay electron spectra, the energy resolution of this dipole beamline was set to a medium value of ∼0.4 eV at the N1s edge. X-ray absorption spectra (XAS; see Supporting Information) were acquired with a standard partial electron yield detector, X-ray photoelectron spectroscopy (XPS), as well as decay electron spectra with a hemispherical electron energy analyzer (Scienta R3000). Sample temperatures were always 300 K. The cleanliness of the samples was checked by XPS. C1s, N1s, and S2p binding energies agreed well with previous measurements.[22,23] XAS results complied with results of previous studies from which tilt angles of the C−N axis with respect to the surface normal of 65 and 60 ± 5° were obtained for C16CN[28] and C2CN,[22] respectively (see Supporting Information for further details).

For the ideal geometry of the C2CN moiety (i.e., at low temperature and without further intermolecular interactions), the orbitals representing the π^* resonances can be labeled according to their orientation with respect to the plane defined by the aliphatic planar C−C−C conformation structure. Their nodal planes are either perpendicular ($[N1s]\pi^*_1$ at 399.6 eV) or parallel to this plane ($[N1s]\pi^*_2$ at 399.7 eV). For SAMs, the aliphatic backbones (and the terminal groups; see above) are commonly tilted with respect to the surface normal (see, e.g., refs 27 and 29). In addition, twisting around the molecular axes of the tilted molecules is possible.[29] XAS and decay electron spectra were recorded for two different polarizations of the light, A_z and A_{xy}. In A_{xy} polarization (normal incidence), the **E** vector of the radiation was oriented perpendicular to the surface normal (see Figure 1b). Taking the random orientation of domains into account by averaging azimuthally around the surface normal and correcting for the tilt angle of 60° and the small cross section differences due to slightly different resonance energies but assuming zero twist angle, we expect an excitation ratio of 4.3 to 1 for $[N1s]\pi^*_2$ compared to $[N1s]\pi^*_1$ for C2CN for this polarization (see Supporting Information for details). The A_z polarization experiments were carried out with a grazing incidence photon beam to give an **E** vector tilted by 10° with respect to the surface normal (Figure 1b); therefore, the excitation of $[N1s]\pi^*_1$ should be favored by a factor of 49.

A nonzero twist angle would reduce this contrast because then, the C−C−C planar symmetry is broken, thereby reducing the difference between $[N1s]\pi^*_1$ and $[N1s]\pi^*_2$ contributions in the XAS signals. For a 60° tilt and a 30° twist, we expect $[N1s]\pi^*_1$ and $[N1s]\pi^*_2$ intensity ratios of 2.3/1 and 1/1.9 for A_z and A_{xy} light, respectively. Because the exact average and distribution of the molecular twist angles are not known, it is problematic to make accurate predictions at present.

Figure 1b shows the decay electron spectra used for the CHC analysis. For the two polarizations, measured decay spectra of C2CN for π-resonant excitation were reproduced by linear combinations of pure resonant and pure nonresonant line shapes, both normalized to unit area. Contributions from direct photoemission have been subtracted. We obtained pure resonant spectra from resonantly excited C16CN samples with 16 methylene spacer units. Because the charge-transfer times in alkanethiols increase exponentially with increasing chain length,[23] no charge delocalization is expected within the investigated time scale for chains with more than four methylene units. Furthermore, for long chains like C16CN, the resonance energy shifts below the Fermi energy, thus making charge transfer from the CN group to the substrate energetically forbidden.[22] The nonresonant spectra recorded 5 eV above the resonance show maxima around 360 (A2) and 377 eV (A1) (see Figure 1b). These belong to two-hole final states, with both holes in outer and holes in inner and outer orbitals, respectively. In the resonant spectra, these maxima (SP1, SP2) correspond to spectator states that are blue shifted by ∼8 eV. This large spectator shift eases the decomposition of the measured spectra and makes the CN group a favorite choice for CHC studies. The third maximum at the highest kinetic energy (393 eV) (P1) has been assigned to a participator decay process.[22,23] These participator lines correspond energetically to photoemission final states, although often with different vibrational progressions due to the evolution of the conformation during the lifetime of the core hole.[19] Inspecting the traces of Figure 1b, it is evident that the nonresonant fraction (green trace) that indicates charge transfer to the substrate before core hole decay is larger for A_z (nearly exclusively $[N1s]\pi^*_1$) than that for A_{xy} ($[N1s]\pi^*_2$ dominates).

From the ratios of resonant and nonresonant intensities ($I_{resonant}/I_{nonresonant}$) of 2.58 ± 0.15 for $[N1s]\pi^*_1$ and 3.28 ± 0.15 for $[N1s]\pi^*_2$ and the lifetime τ_{core} of the N1s core hole of 6.4 fs,[30] we obtain averaged charge-transfer times of two independent data sets of 16.5 and 21.0 fs. These turn into (i) 15.9 fs for $[N1s]\pi^*_1$ and 22.2 fs for $[N1s]\pi^*_2$ after applying the above-mentioned excitation energy and tilt angle correction and (ii) 11.7 and 26 fs after considering in addition a twist angle of 30°. We note that correction (i) is well-justified by experimental and theoretical results (see below). The twist angle of the SAMs, on the other hand, is not known. The estimate for correction (ii) shows, however, that such a possible geometry effect would increase the intrinsic contrast but not cause any decrease.

It is remarkable that the transfer of the resonantly excited electron is faster for the $[N1s]\pi^*_1$ state despite its smaller resonance energy by 0.1 eV. We also note the good reproducibility of the CHC results for this material; measurements from different preparations and at three different experimental stations yielded values for the charge-transfer time between 14 and 16.5 fs for A_z polarization.[22,23] We further note that the total error of ±4 fs in refs 22 and 23 is mainly governed by the uncertainty of τ_{core}, which does not enter the comparison made here, whereas the error of determining the ratio $I_{resonant}/I_{nonresonant}$ is due to the fitting procedure and is estimated to be ±0.15, which contributes with ±1 fs to the total error of the charge-transfer times.

To elucidate the ET mechanism and the origin of the different electron injection times, we have simulated the ET process using a protocol that combines electronic structure calculations at the density functional theory (DFT) level with quantum dynamics simulations (see refs 31−33 and Supporting Information for details). The ET dynamics simulation is performed using a diabatic representation where the (quasi)-diabatic basis is constructed using charge-localized electronic states relevant for the process. For the particular case discussed in this work, these states are the donor state, $|\psi_d\rangle$, that corresponds (in the vanishing coupling limit) to the product of

dx.doi.org/10.1021/jz2015567 | J. Phys. Chem. Lett. 2012, 3, 436−440

an excited state localized in the photoabsorbing tailgroup and an empty band of the metal surface and a quasi-continuum set of acceptor states, $|\psi_a\rangle$, corresponding (in the zero coupling limit) to the product of the ground state of the cation of the donor and a band state of the metal that gets populated as a consequence of the ET. In this basis, the Hamiltonian for the electronic dynamics takes the form

$$\hat{H} = |\psi_d\rangle E_d \langle\psi_d| + \sum_a |\psi_a\rangle E_a \langle\psi_a| + \sum_a (|\psi_d\rangle V_{da} \langle\psi_a| + |\psi_a\rangle V_{ad} \langle\psi_d|) \quad (1)$$

where E_d and E_a, the diagonal elements of the diabatic potential matrix, are the energies of the donor and acceptor states involved in the ET process, respectively, and the off-diagonal elements, V_{ad}, are the donor−acceptor ET coupling terms. The parameters used in the ET Hamiltonian (the donor and acceptor energies and the coupling terms; see eq 1) have been obtained using a partitioning method. The Hamiltonian and the molecular orbitals needed in the partitioning technique have been calculated using a mean-field single-electron approach based on DFT methods for a cluster model of the extended system (see Supporting Information for the details). To this end, in the first step of the procedure, we have determined the adsorption geometry of the organic molecule at the Au surface in the low coverage limit using periodic calculations. It was found that the most stable geometry is fcc bridge-like with the C−N axis tilted 70.7° with respect to the surface normal (see Figure 2), in reasonable agreement with the experimental value.

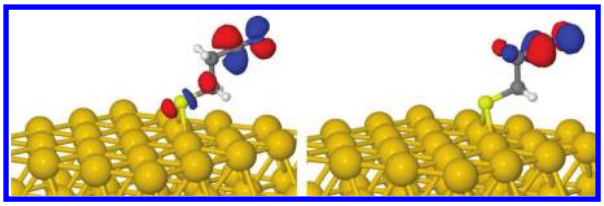

Figure 2. Orbitals representing the π^*_1 (left) and π^*_2 (right) donor states.

We note that for this geometry, the twist angle would be 0. In the second step, we have determined the donor and acceptor states and the donor−acceptor couplings using a cluster model obtained from the periodic calculations. These parameters have subsequently been employed for the simulation of the electron injection dynamics process using eq 1. In all calculations, the polarizing effect of the N1s core hole has not been taken into account. This may affect the energetics and extension of the orbitals and can cause quantitative discrepancies with the experimental injection times. However, it is expected that the π^*_1 and π^*_2 resonances are influenced in a similar way by the core hole, and therefore, the qualitative difference in the mechanism underlying the charge-transfer process from the π^*_1, π^*_2 donor orbitals should not be altered by including the core hole. Figure 2 shows orbitals representing the π^*_1 and π^*_2 donor states. The π^*_1 state exhibits contributions not only at the nitrile group but also on the aliphatic backbone as well as at the sulfur atom of the thiolate bond. The π^*_2 state, on the other hand, is localized at the nitrile group and the hydrogen atoms of the upper methylene group of the backbone, that is, it has negligible density at atoms close to the substrate. The significant contribution at the aliphatic bridge causes a stronger donor−acceptor coupling for the π^*_1 state, which results in the different ET times of the two donor states. The simulation of the electron injection dynamics reveals ET times of 3.8 fs for the π^*_1 state and 46.8 fs for the π^*_2 state, giving a factor of ∼12 increase in the rate due to orbital overlap. These results reproduce the experimentally observed trend within the limitations of the model used. In particular, the model neither takes into account the possible existence of defects in the Au surface, which may modify the type of binding of the organic molecule, nor includes temperature-related effects. Thermal excitation can cause, for example, a non-negligible population of nonplanar C−C−C configurations, which may influence the ET dynamics through the C−C−C unit. This would, in the limit of an average rotation twist of the CN group, completely break the symmetry of the overlap geometry and give a single value of the lifetime, which is not observed.

In summary, we have demonstrated by applying the CHC method that charge transport in organic layers can depend on the initially excited resonance state even in cases where the energy separation of the respective states is much smaller than their width so that selective excitation is only possible by exploiting symmetry. Calculations explain this effect by the different shape of the orbitals representing the resonance states, in particular, their extensions onto the backbone and head group. We believe that this technique is applicable to a large variety of systems with negligible energy splitting, for example, functional groups attached to alkane chains. Because the activation energy for gauche defects is low in alkanes (less than 4 kJ/mol[34]), we expect even larger contrast at sample temperatures lower than 300 K, for which the perfect antiperiplanar configuration is more likely.

■ ASSOCIATED CONTENT

Supporting Information

Details on the sample characterization, the determination of the polarization ratios, and theoretical methods. This material is available free of charge via the Internet at http://pubs.acs.org.

■ AUTHOR INFORMATION

Corresponding Author

*E-mail: florian.blobner@ph.tum.de. Phone: +49 (0) 89 289 12627. Fax: +49 (0) 89 289 12338 (F.B.); E-mail: pedro.brana-coto@physik.uni-erlangen.de. Phone: 49 (0) 9131 85 28816. Fax: 49 (0) 9131 85 28833 (P.B.C.).

Notes

The authors declare no competing financial interest.

■ ACKNOWLEDGMENTS

We thank K. Diller, A. Papageorgiou, A. Nefedov, and the staff of BESSY for help during the experiments and Ch. Wöll (KIT) for the use of the experimental station. F.B., F.A., and P.F. thank J.V. Barth, the DFG cluster of excellence Munich Centre for Advanced Photonics (Project C.1.8.), and the Helmholtz-Zentrum-Berlin for financial support and J. Reichert and D. Menzel for valuable discussions. M.Z. thanks DFG (ZH 63/14-1) for support of this work. M.T., O.R.P., and P.B.C. thank the Munich Centre for Advanced Photonics (Project C.1.6) and the BMBF for support of this work. H.W. acknowledges support from the National Science Foundation (CHE-1012479). Computing time provided by the Jülich Supercomputing Centre and the Leibniz Rechenzentrum München is gratefully acknowledged.

REFERENCES

(1) Weissman, S. I. Intramolecular Electron Exchange in Anions of Paracyclophanes. *J. Am. Chem. Soc.* **1958**, *80*, 6462−6463.
(2) Voevodskij, V.; Solodovnikov, S.; Chibrikin, V. *Dokl. Akad. Nauk S.S.S.R.* **1959**, *129*, 1082.
(3) McConnell, H. Intramolecular Charge Transfer in Aromatic Free Radicals. *J. Chem. Phys.* **1961**, *35*, 508−515.
(4) Marcus, R.; Sutin, N. Electron Transfer in Chemistry and Biology. *Biochim. Biophys. Acta* **1985**, *811*, 265−322.
(5) Bixon, M.; Jortner, J. *Advances in Chemical Physics*; John Wiley & Sons, Inc.: New York, 2007; pp 35−202.
(6) Barbara, P.; Meyer, T.; Ratner, M. A. Contemporary Issues In Electron Transfer Research. *J. Phys. Chem.* **1996**, *100*, 13148−13168.
(7) Itoh, N.; Stoneham, A. M. *Materials Modification by Electronic Excitation*; Cambridge University Press: Cambridge, U.K., 2001.
(8) Zharnikov, M.; Frey, S.; Heister, K.; Grunze, M. Modification of Alkanethiolate Monolayers by Low Energy Electron Irradiation: Dependence on the Substrate Material and on the Length and Isotopic Composition of the Alkyl Chains. *Langmuir* **2000**, *16*, 2697−2705.
(9) Williams, D. B.; Carter, C. B. *Transmission Electron Microscopy*; Springer: Berlin, Germany, 2009.
(10) Duncan, W. R.; Prezhdo, O. V. Theoretical Studies of Photoinduced Electron Transfer in Dye-Sensitized TiO_2. *Annu. Rev. Phys. Chem.* **2007**, *58*, 143−184.
(11) Hagfeldt, A.; Boschloo, G.; Sun, L.; Kloo, L.; Pettersson, H. Dye-Sensitized Solar Cells. *Chem. Rev.* **2010**, *110*, 6595−6663.
(12) Cuevas, J.; Scheer, E. *Molecular Electronics*; World Scientific Series in Nanoscience and Nanotechnology; World Scientific: Singapore, 2010; Vol. *1*.
(13) Haick, H.; Cahen, D. Making Contact: Connecting Molecules Electrically to the Macroscopic World. *Prog. Surf. Sci.* **2008**, *83*, 217−261.
(14) Lindsay, S.; Ratner, M. A. Molecular Transport Junctions: Clearing Mists. *Adv. Mater.* **2007**, *19*, 23−31.
(15) Secker, D.; Wagner, S.; Ballmann, S.; Hartle, R.; Thoss, M.; Weber, H. B. Resonant Vibrations, Peak Broadening, and Noise in Single Molecule Contacts: The Nature of the First Conductance Peak. *Phys. Rev. Lett.* **2011**, *106*, 136807.
(16) Tsutsui, M.; Taniguchi, M.; Kawai, T. Single-Molecule Identification via Electric Current Noise. *Nat. Commun.* **2010**, *1*, 138.
(17) Campbell, J. L.; Papp, T. Widths of the Atomic K-N7 Levels. *Atom. Data Nucl. Data Tables* **2001**, *77*, 1−56.
(18) Björneholm, O.; Nilsson, A.; Sandell, A.; Hernnäs, B.; Mårtensson, N. Determination of Time Scales for Charge Transfer Screening in Physisorbed Molecules. *Phys. Rev. Lett.* **1992**, *68*, 1892−1895.
(19) Brühwiler, P. A.; Karis, O.; Mårtensson, N. Charge-Transfer Dynamics Studied Using Resonant Core Spectroscopies. *Rev. Mod. Phys.* **2002**, *74*, 703−740.
(20) Wang, L.; Chen, W.; Wee, A. T. S. Charge Transfer Across the Molecule/Metal Interface Using the Core Hole Clock Technique. *Surf. Sci. Rep.* **2008**, *63*, 465−486.
(21) Menzel, D. Ultrafast Charge Transfer at Surfaces Accessed by Core Electron Spectroscopies. *Chem. Soc. Rev.* **2008**, *37*, 2212−2223.
(22) Neppl, S.; Bauer, U.; Menzel, D.; Feulner, P.; Shaporenko, A.; Zharnikov, M.; Kao, P.; Allara, D. Charge Transfer Dynamics in Self-Assembled Monomolecular Films. *Chem. Phys. Lett.* **2007**, *447*, 227−231.
(23) Kao, P.; Neppl, S.; Feulner, P.; Allara, D. L.; Zharnikov, M. Charge Transfer Time in Alkanethiolate Self-Assembled Monolayers via Resonant Auger Electron Spectroscopy. *J. Phys. Chem. C* **2010**, *114*, 13766−13773.
(24) Ballav, N.; Schüpbach, B.; Neppl, S.; Feulner, P.; Terfort, A.; Zharnikov, M. Biphenylnitrile-Based Self-Assembled Monolayers on Au(111): Spectroscopic Characterization and Resonant Excitation of the Nitrile Tail Group. *J. Phys. Chem. C* **2010**, *114*, 12719−12727.
(25) Hamoudi, H.; Neppl, S.; Kao, P.; Schüpbach, B.; Feulner, P.; Terfort, A.; Allara, D.; Zharnikov, M. Orbital-Dependent Charge Transfer Dynamics in Conjugated Self-Assembled Monolayers. *Phys. Rev. Lett.* **2011**, *107*, 027801.
(26) Deppe, M.; Föhlisch, A.; Hennies, F.; Nagasono, M.; Beye, M.; Sánchez-Portal, D.; Echenique, P. M.; Wurth, W. Ultrafast Charge Transfer and Atomic Orbital Polarization. *J. Chem. Phys.* **2007**, *127*, 174708.
(27) Love, J. C.; Estroff, L. A.; Kriebel, J. K.; Nuzzo, R. G.; Whitesides, G. M. Self-Assembled Monolayers of Thiolates on Metals as a Form of Nanotechnology. *Chem. Rev.* **2005**, *105*, 1103−1169.
(28) Frey, S.; Shaporenko, A.; Zharnikov, M.; Harder, P.; Allara, D. L. Self-Assembled Monolayers of Nitrile-Functionalized Alkanethiols on Gold and Silver Substrates. *J. Phys. Chem. C* **2003**, *107*, 7716−7725.
(29) Schreiber, F. Structure and Growth of Self-Assembling Monolayers. *Prog. Surf. Sci.* **2000**, *65*, 151−256.
(30) Kempgens, B.; Kivimäki, A.; Neeb, M.; Köppe, H. M.; Bradshaw, A. M.; Feldhaus, J. A High-Resolution N 1s Photoionization Study of the N_2 Molecule in the Near-Threshold Region. *J. Phys. B: At. Mol. Opt. Phys.* **1996**, *29*, 5389.
(31) Kondov, I.; Cizek, M.; Benesch, C.; Wang, H.; Thoss, M. Quantum Dynamics of Photoinduced Electron-Transfer Reactions in Dye-Semiconductor Systems: First-Principles Description and Application to Coumarin 343−TiO_2. *J. Phys. Chem. C* **2007**, *111*, 11970−11981.
(32) Li, J.; Nilsing, M.; Kondov, I.; Wang, H.; Persson, P.; Lunell, S.; Thoss, M. Dynamical Simulation of Photoinduced Electron Transfer Reactions in Dye-Semiconductor Systems with Different Anchor Groups. *J. Phys. Chem. C* **2008**, *112*, 12326−12333.
(33) Li, J.; Kondov, I.; Wang, H.; Thoss, M. Theoretical Study of Photoinduced Electron-Transfer Processes in the Dye-Semiconductor System Alizarin−TiO_2. *J. Phys. Chem. C* **2010**, *114*, 18481−18493.
(34) McMurray, J. *Organic Chemistry*; Brooks/Cole: Florence, KY, 2007.